ADVANCED FUNCTIONAL MATERIALS



DOI: 10.1002/adfm.200700953

# Controlled Synthesis of $Ag_2S$, $Ag_2Se$, and Ag Nanofibers by Using a General Sacrificial Template and Their Application in Electronic Device Fabrication**

By *Hailiang Wang* and *Limin Qi**

Nanofiber bundles of $Ag_2S$, $Ag_2Se$, and Ag have been successfully synthesized by making use of $Ag_2C_2O_4$ template nanofiber bundles, utilizing both anion-exchange and redox reactions. The obtained bundles were polycrystalline nanofibers composed of nanoparticles in which the precursor morphology was well-preserved, indicating that $Ag_2C_2O_4$ nanofiber bundles acted as a general sacrificial template for the synthesis of silver-based semiconductor and metal nanofibers. Dispersing media and transforming reactants were found to be key factors influencing the chemical transformation in the system. In particular, separate single-crystalline Ag nanofibers were obtained via a nontemplate route when ascorbic acid was used as a relatively weak reductant. An electrical transfer and switching device was built with the obtained $Ag_2S$ and Ag nanofiber bundles, utilizing the unique ion-conductor nature of $Ag_2S$ and revealing their potential applications in electronics.

## 1. Introduction

The template method is an effective approach for the controlled synthesis of nanomaterials with various morphologies and has attracted a lot of efforts.[1–4] Hard templates such as polymer or anodic aluminum oxide (AAO) membranes,[3] mesoporous silica,[5] and colloid crystals[6] as well as soft templates including surfactants,[7] polymers,[8] DNA chains,[9] and micro-organisms[10,11] have been widely used for this purpose. However, harsh conditions or complicated procedures are required to remove these templates. Sacrificial templates, which act as both reactive precursors and templates, are not only free from the template removal problem but also from the limited morphologies of hard templates, because the precursors can be fabricated through all the techniques developed for morphosynthesis of nanomaterials.[4,12–16] Intrigued by many encouraging results obtained from sacrificial-template-based morphosynthesis in solution, employing either ion exchange[16,17] or redox[15,18] reactions, we attempt to extend this method by transforming the same precursor with these two kinds of chemical reactions.

$Ag_2S$ is a useful semiconductor and solid ionic conductor, conducting both ions and electrons at room temperature;[19–21] $Ag_2Se$ is an important semiconductor with promising thermoelectric properties, large magnetoresistance, and high electrical conductivity;[14b,22] Ag has the highest electrical and thermal conductivity among all the metals.[23] Their 1D nanomaterials are important functional or connecting elements in nanometer-scale device fabrication[24–27] with tremendous applications in electronics. For example, Hasegawa and co-workers[24] have realized atomic switches using $Ag_2S$-coated Ag nanowires. However, nanowire-like $Ag_2S$ is still difficult to synthesize. Successful approaches in literature include electrochemical reactions using AAO templates[25,28] and silver-substrate-assisted reactions,[20] but both the membrane and the substrate need to be removed for pure $Ag_2S$ nanowires and these methods are suitable for large-scale synthesis. Although solution processing has been achieved recently under sonication,[29] the resulted $Ag_2S$ nanowires were amorphous. Therefore, the preparation of 1D $Ag_2S$, $Ag_2Se$, and Ag nanomaterials from one system with good crystallinity is challenging.

Herein, we report a facile synthesis of $Ag_2S$, $Ag_2Se$, and Ag nanofiber bundles by making use of $Ag_2C_2O_4$ template nanofiber bundles obtained from polymer-directed crystallization, employing both anionic exchange and redox reactions. While all the templated nanofibers were 1D nanoparticle assemblies with a polycrystalline nature, single-crystalline Ag nanofibers could be obtained via a nontemplating route by changing the reducing conditions. Finally, an electrical transportation and switching device was built with the synthesized nanofiber bundles of $Ag_2S$ and Ag, showing potential applications in nanoscale device building and integration.

[*] Prof. L. Qi, H. Wang
Beijing National Laboratory for Molecular Sciences
State Key Laboratory for Structural Chemistry of Unstable and Stable Species
College of Chemistry, Peking University
Beijing 100871 (P.R. China)
E-mail: liminqi@pku.edu.cn

[**] This work was supported by NSFC (20325312, 20673007, 20473003, and 50521201) and MOST (2007CB936201). Supporting Information is available online from Wiley InterScience or from the authors.

## 2. Results and Discussion

In our experiments, $Ag_2C_2O_4$ crystals were synthesized by mixing $Na_2C_2O_4$ and $AgNO_3$ in aqueous solution. In the absence of polymeric additives, rhombohedral and rhombic-plate-like $Ag_2C_2O_4$ crystals were obtained (Fig. S1a and b), resulting from the inherent growth propensity of $Ag_2C_2O_4$ crystals. Elongated $Ag_2C_2O_4$ crystals with sharpening ends could be obtained by slightly changing the concentration of reactants (Fig. S1c). Nevertheless, it is difficult to obtain 1D nanostructures of $Ag_2C_2O_4$ with high aspect ratios by solely changing the reactant concentration. Poly(acrylic acid) (PAA) was introduced to the system because it interacted quite strongly with $Ag^+$ ion and could induce 1D crystal growth.[8d] When 0.5g $L^{-1}$ PAA was added to the solution, the rodlike $Ag_2C_2O_4$ crystals changed into nanofiber bundles (Fig. S1d). After the optimization of synthesis conditions, 1D $Ag_2C_2O_4$ crystals with ultrahigh aspect ratios were obtained in the presence of PAA (Fig. 1). X-ray

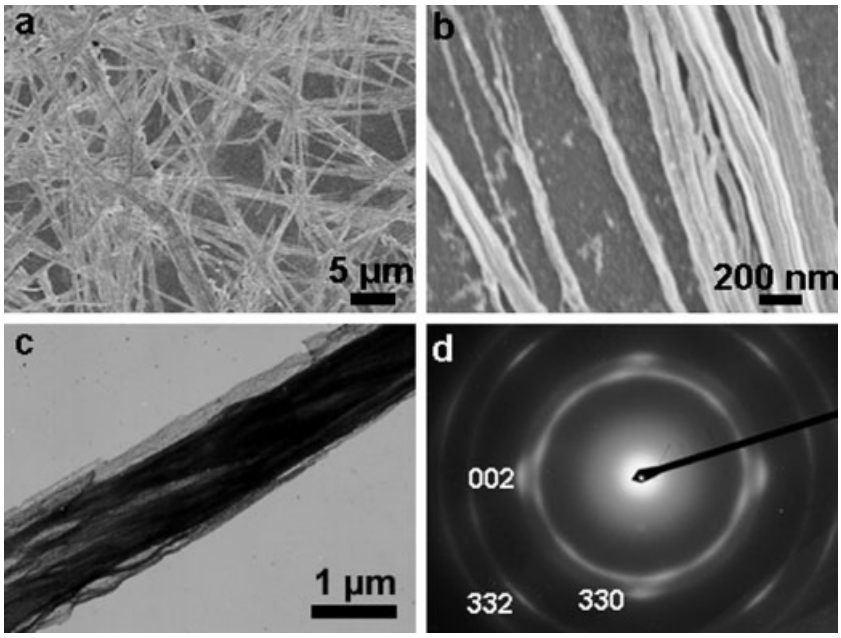


**Figure 1.** a,b) Scanning electron microscopy and c) transmission electron microscopy images, and d) electron diffraction pattern of $Ag_2C_2O_4$ nanofiber bundles obtained in the presence of PAA. $[Na_2C_2O_4] = 1$ mM, $[AgNO_3] = 20$ mM, $[PAA] = 0.5$g $L^{-1}$.

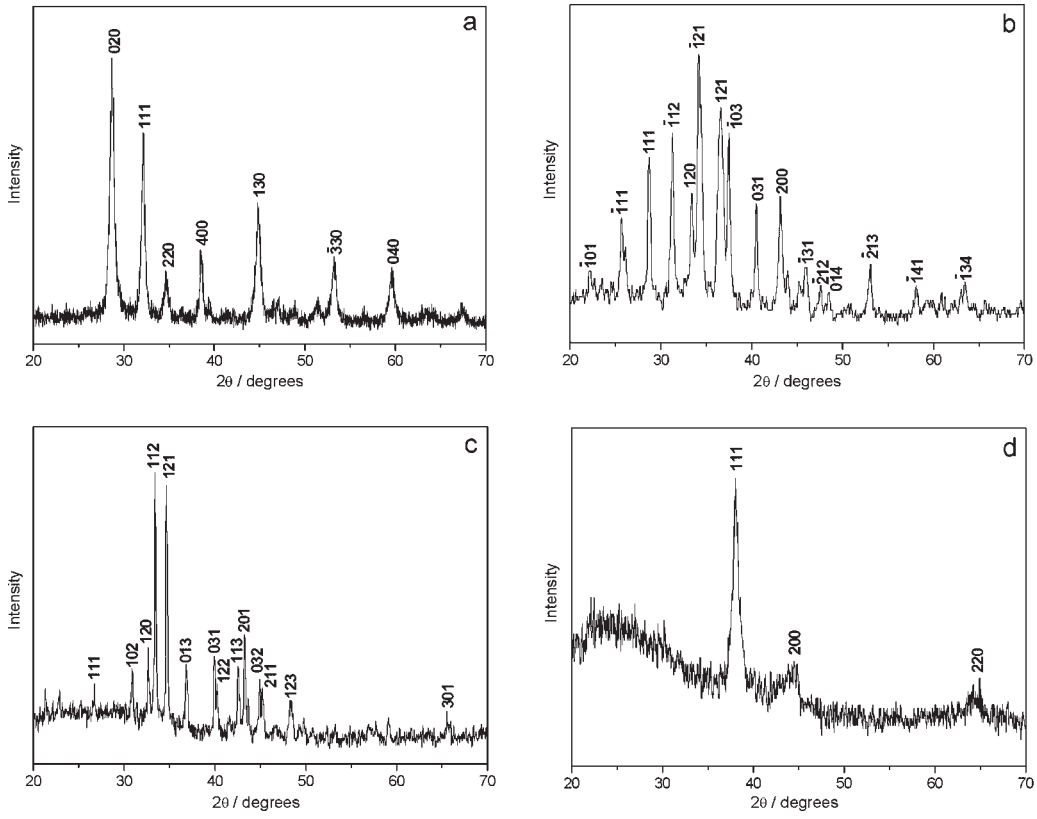


**Figure 2.** XRD patterns of a) $Ag_2C_2O_4$ nanofiber bundles and the templated b) $Ag_2S$, c) $Ag_2Se$, and d) Ag nanofiber bundles.

ADVANCED FUNCTIONAL MATERIALS



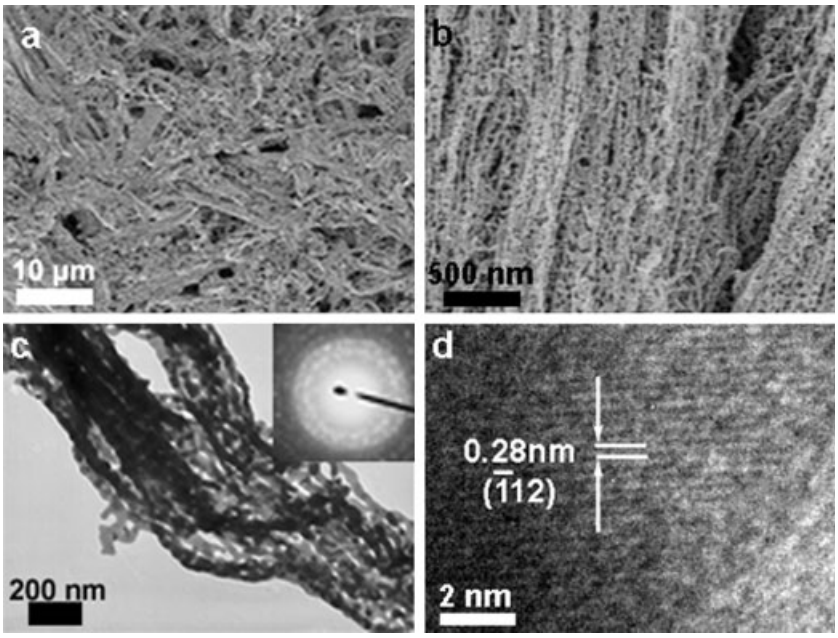


**Figure 3.** a,b) SEM, c) TEM, and d) high-resolution TEM images of $Ag_2S$ nanofiber bundles obtained by templating $Ag_2C_2O_4$ nanofibers. The inset shows the related ED pattern.

diffraction (XRD) analysis (Fig. 2a) indicated that the product comprised pure $Ag_2C_2O_4$ crystals of monoclinic structure (Joint Committee on Powder Diffraction Standards (JCPDS) file number 22-1335). From the scanning electron microscopy (SEM) and transmission electron microscopy (TEM) images shown in Figure 1, it is observed that the $Ag_2C_2O_4$ nanofibers self-aggregated into bundles. The length of the nanofibers is around 100 μm, while the diameter of individual nanofibers is less than 20 nm (Fig. 1b), which corresponds to a very large aspect ratio. Figure 1d shows the electron diffraction (ED) pattern of a bundle of $Ag_2C_2O_4$ nanofibers, indicating a polycrystalline nature with a preferential growth direction normal to the (332) facets.

The $Ag_2C_2O_4$ nanofiber bundles can be chemically transformed to $Ag_2S$, $Ag_2Se$, and Ag nanofibers if proper dispersing medium and reactants are selected. $Ag_2S$ nanofiber bundles could be obtained by mixing thioacetamide (TAA) with the $Ag_2C_2O_4$ precursor in ethanol (Fig. 3). XRD analysis (Fig. 2b) suggested that the $Ag_2C_2O_4$ precursor was completely transformed to monoclinic $\alpha$-$Ag_2S$ (JCPDS 14-0072). The morphology of the nanofiber bundles was retained in a large scale, as evidenced by the low-magnification SEM image in Figure 3a. The diameter of an individual $Ag_2S$ nanofiber was measured to be about 20 nm from high-magnification SEM and TEM images (Fig. 3b and c), which agrees well with the diameter of the original $Ag_2C_2O_4$ nanofibers. Moreover, it is noted that the $Ag_2S$ nanofibers are composed of nanoparticles, which leads to the polycrystalline ED pattern (Fig. 3c, inset). Further electron diffraction investigation of a single nanofiber showed that the ED pattern exhibits relatively weak, discontinuous rings instead of clear spots, demonstrating that each nanofiber is polycrystalline rather than single-crystalline, which is consistent with the apparent morphology of the nanofibers consisting of primary nanocrystals. A high-resolution transmission electron microscopy (HRTEM) image (Fig. 3d) displays clear lattices of $Ag_2S$ crystal, confirming that the product was crystalline $Ag_2S$ nanofibers. The product displayed an absorption peak at about 530 nm in the UV-vis region (Fig. 4a), considerably blue-shifted compared to the band gap of bulk $Ag_2S$ (1 eV, 1240 nm),[30] indicating that the nanofibers were aggregates of nanoparticles within the quantum confinement regime. In addition, the structural defects of the obtained $Ag_2S$ nanofibers could also contribute to the observed blue shift. The spectrum also showed a broad absorption into the near-IR region, possibly due to scattering by large nanofiber bundles or absorption by some large coalescing aggregates. The influence of dispersing medium on the chemical transformation of $Ag_2C_2O_4$ nanofiber bundles was investigated. It was observed that the morphology of precursor was

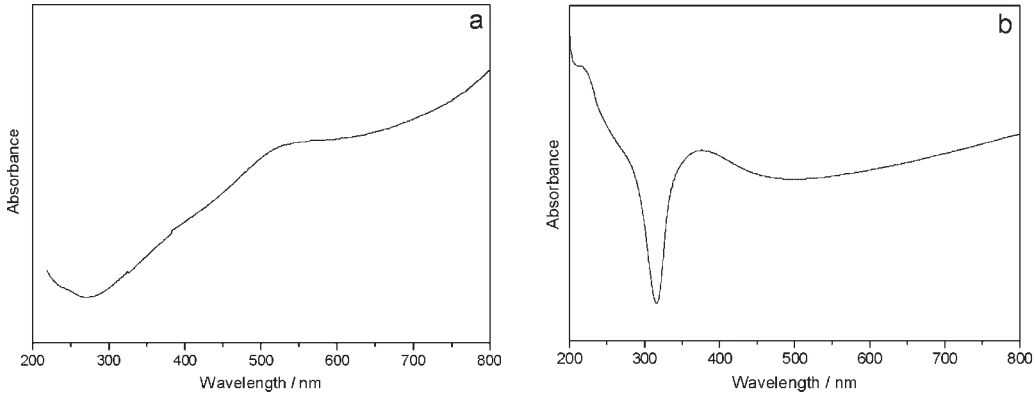


**Figure 4.** UV-vis absorption spectra of a) $Ag_2S$ and b) Ag nanofiber bundles obtained by templating $Ag_2C_2O_4$ nanofibers.

  

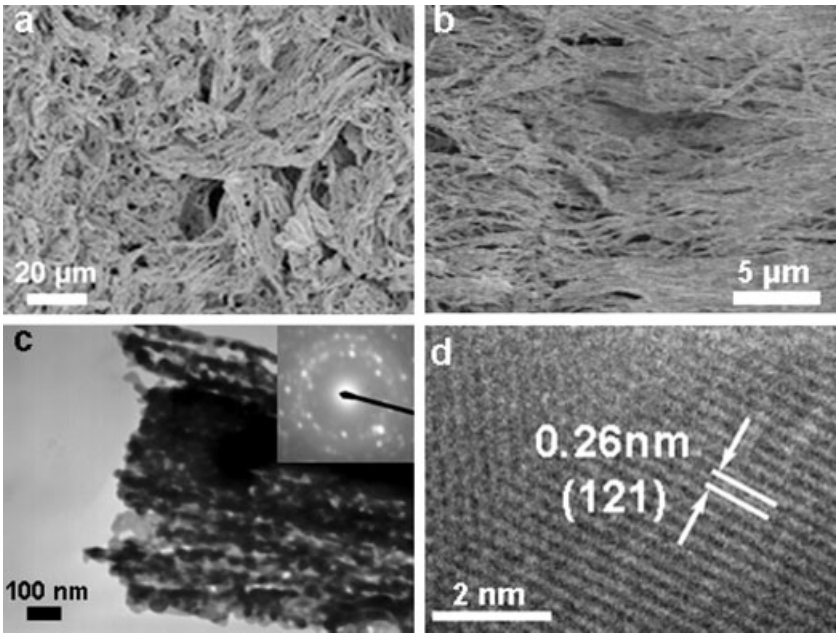


**Figure 5.** a,b) SEM, c) TEM, and d) HRTEM images of $Ag_2Se$ nanofiber bundles obtained by templating $Ag_2C_2O_4$ nanofibers. The inset in (c) shows the related ED pattern.

more likely to be retained when dispersed in ethanol than water (Fig. S2), which may be rationalized by considering that the insolubility of $Ag_2C_2O_4$ in ethanol favored a direct reaction between TAA and $Ag_2C_2O_4$ rather than a reaction between TAA and dissolved $Ag^+$ ions.

Similarly, $Ag_2Se$ nanofiber bundles were obtained by mixing $Na_2SeSO_3$ with the $Ag_2C_2O_4$ precursor dispersed in water (Fig. 5). The XRD pattern of the transformed product (Fig. 2c) exhibited reflections characteristic of orthorhombic $\beta$-$Ag_2Se$ (JCPDS 24-1041), confirming a complete transformation from $Ag_2C_2O_4$ to $Ag_2Se$. Like the case of $Ag_2S$, the obtained $Ag_2Se$ nanofibers were also composed of nanoparticles and thus polycrystalline (Fig. 5c). The HRTEM image shown in Figure 5d displays clear lattices of $Ag_2Se$ crystal, confirming the formation of crystalline $Ag_2Se$ nanofibers. It is noted that the diameter of a single $Ag_2Se$ nanofiber was about 50–100 nm (Fig. 5b and c), which was much larger than that of the $Ag_2C_2O_4$ precursor. This could be due to aggregation between several $Ag_2C_2O_4$ nanofibers during chemical transformation. Unlike the case of $Ag_2S$, transcription to $Ag_2Se$ in ethanol gave very similar results as in water, which may be ascribed to the fast reaction between $Na_2SeSO_3$ and $Ag_2C_2O_4$ in both in ethanol and water.

Besides anionic exchange reactions, the $Ag_2C_2O_4$ template is also suitable for reduction so that the product of our chemical transformation can be extended from silver-based semiconductors to metal nanofibers. Using $NaBH_4$ as reductant and water as dispersing medium, the $Ag_2C_2O_4$ nanofiber bundles could be transformed to Ag with preservation of their morphology (Fig. 6). XRD analysis (Fig. 2d) suggested that the product was pure face-centered-cubic Ag (JCPDS 04-0783). It is noted that the diffraction peaks were considerably broadened because these nanofibers were nanoparticle assemblies. The diameter of these nanoparticles was calculated to be about 12 nm from the (111) diffraction peak according to the Scherrer equation, in good agreement with the TEM data. The Ag nanofibers in the bundles had an average diameter of less than 20 nm. Although the Ag nanofibers

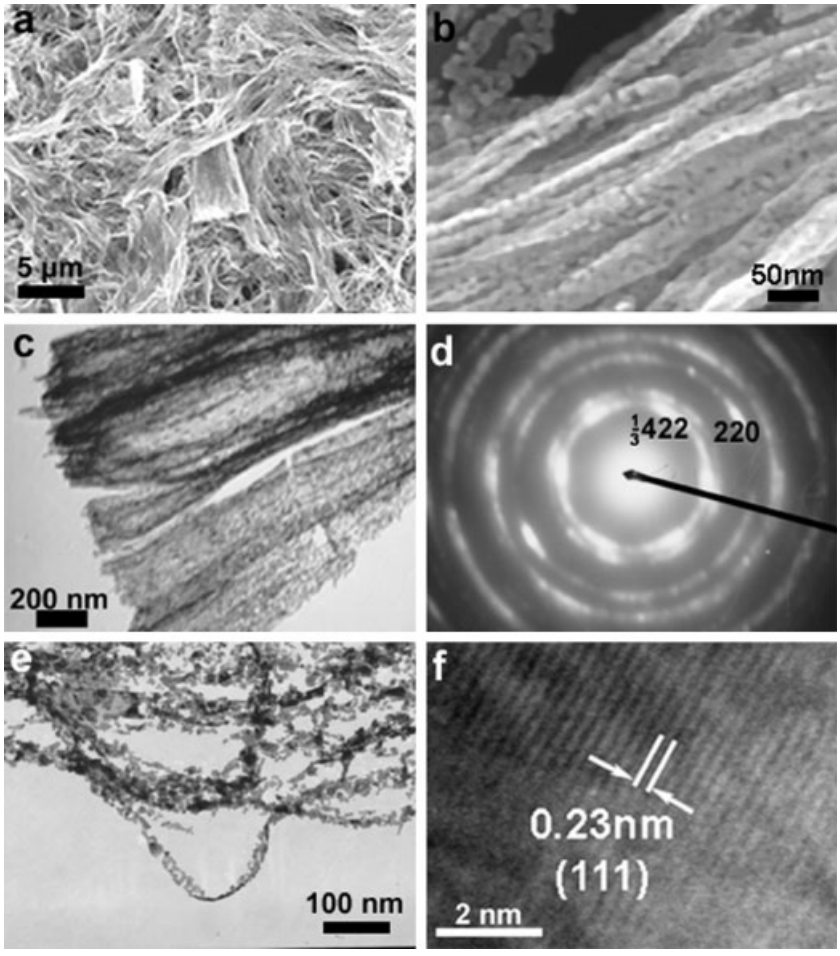


**Figure 6.** a,b) SEM, c,e) TEM, and f) HRTEM images of Ag nanofiber bundles obtained by templating $Ag_2C_2O_4$ nanofibers. Panel (d) shows the related ED pattern of nanofiber bundles in (c).

were composed of nanoparticles similar to those of $Ag_2S$ and $Ag_2Se$ (Fig. 6c and e), the ED pattern (Fig. 6d) related to the nanofiber bundles shown in Figure 6c suggested their polycrystalline nature with a preferential orientation along the [110] direction. It should be noted that the preferentially oriented polycrystalline nature of the $Ag_2C_2O_4$ precursor was kept after reduction reaction, possibly because of certain structural matching between $Ag_2C_2O_4$ and Ag crystals or inherent tendency of [110]-oriented attachment of Ag nanocrystals. Considering that there is no obvious matching between the $d$(332) spacing of the $Ag_2C_2O_4$ crystals (1.17 Å) and the $d$(220) spacing of the Ag crystals (1.445 Å), it seems more reasonable that the 1D aggregation and growth tendency along the Ag [110] direction under the current reaction condition could lead to the formation of the Ag nanofiber bundles with a preferential orientation along the [110] direction. As is to be mentioned below, the Ag nanofibers obtained directly from solution did not form tight bundles and their growth directions were not limited to the [110] direction, which ruled out a dissolution–reconstruction process for the current transformation. Therefore, it may be reasonably deduced that the $Ag_2C_2O_4$ nanofibers actually acted as a precursor template for the direct transformation into polycrystalline Ag nanofibers with a preferential [110] orientation although the exact reason for the preferential orientation is not well understood. In the literature, there are quite a few examples of chemical transformation between single crystals; however, most of them utilized ion exchange reactions, in which the lattice of either the cation or anion did not change and thus could hold the nanostructures intact. Here we achieved redox transformation between preferentially-oriented polycrystals for the first time, which would provide useful information for controlled synthesis of 1D nanostructures through chemical transformation of precursor templates. Nevertheless, the exact mechanism for the transformation between preferentially- oriented polycrystalline nanofibers remains to be fully elucidated.

To investigate the surface plasmon resonance (SPR) of the obtained Ag nanofiber bundles, UV-vis spectroscopy was carried out. As shown in Figure 4b, the absorption peak was observed at 376 nm, which was blue-shifted compared to well-dispersed Ag nanocrystals, mainly owing to the small particle size and 1D aggregation effect. It has been reported that Ag nanoparticles with an average diameter of 21 nm display an SPR absorption at 410 nm.[31] Since the nanoparticles forming the Ag nanofibers had an average diameter of 12 nm, the absorption peak would blue-shift because of smaller diameter. On the other hand, the Ag nanoparticles arranged themselves into 1D nanofibers and were very closely packed, which would further blue-shift their SPR absorption, as indicated by calculation with Mie's theory.[32] This phenomenon is reminiscent of our previous finding that Ag nanoparticles with 1D arrangement before coalescing into nanowires displayed an SPR absorption at 377 nm.[33]

Interestingly, separate Ag nanofibers instead of nanofiber bundles were obtained when the $Ag_2C_2O_4$ nanofibers were dispersed in a larger volume of water and reduced with ascorbic acid (Vc) at 4 °C (Fig. 7). The SEM image shown in Figure 7a suggested that there were no bundles and the TEM images shown in Figure 7b–e suggested that each separate Ag nanofiber had a diameter of about 50 nm. According to the TEM and ED analysis of a large number of Ag nanofibers, it was revealed that the separate Ag nanofibers were actually single crystals grown along the four different directions: [110], [211], [100], and [111]. While the first two are common in the

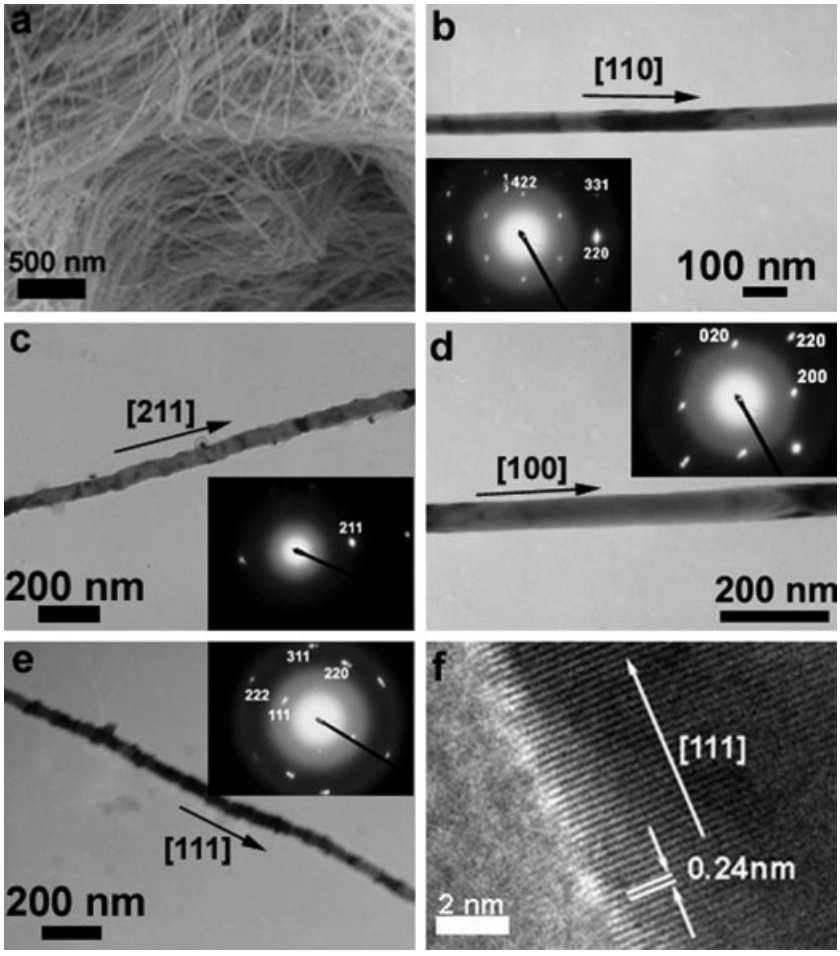


**Figure 7.** a) SEM, b–e) TEM, and f) HRTEM images of separate Ag nanofibers obtained by reducing the $Ag_2C_2O_4$ nanofiber dispersion with ascorbic acid. The insets show the related ED patterns.

literature,[34] the latter two have been rarely observed. The HRTEM image shown in Figure 7f displayed clear (111) crystal lattices of a [111]-oriented Ag nanofiber.

It is noticed that the separate Ag nanofibers obtained by using Vc as the reductant are apparently different from the original $Ag_2C_2O_4$ template or the Ag nanofiber bundles obtained by using $NaBH_4$ as the reductant in that they are well-separated single crystals with larger diameters. We speculate that the separate Ag nanofibers were not produced following the direct-template mechanism. It is known that $Ag_2C_2O_4$ is sparsely soluble in water and the $Ag^+$ ions are easier to be reduced than $Ag_2C_2O_4$ crystals. When the $Ag_2C_2O_4$ precursor was reduced with Vc whose reducing ability is weaker than $NaBH_4$, $Ag^+$ ions in water were first reduced and the $Ag_2C_2O_4$ crystals had enough time to dissolve into water, providing enough $Ag^+$ ions in water as the main Ag source for reduction. In the case of $NaBH_4$, the rapid reduction reaction exceeded the equilibrium recovery of $Ag_2C_2O_4$ dissolution, and thus the product retained the morphology of the precursor as the crystals were the main Ag source. Control experiments were carried out to test the above speculation. After dispersing the $Ag_2C_2O_4$ precursor in water, $HNO_3$ was dropped in until the precipitate completely dissolved. Then NaOH was added till the pH of the solution returned to the pH value similar to that before adding $HNO_3$ but the solution was still clear. The next steps for chemical transformation were the same with the normal transformations. As expected, while none of the $Ag_2S$, $Ag_2Se$, and Ag nanofiber bundles could be obtained, separate Ag nanofibers were readily obtained when Vc was used as the reductant. This led to the conclusion that the formation of separate Ag nanofibers resulted from the reduction of $Ag^+$ ions in solution whereas the formation of $Ag_2S$, $Ag_2Se$, and Ag nanofiber bundles resulted from the anionic exchange/reduction of the $Ag_2C_2O_4$ nanofiber bundles, following a direct-template mechanism.

An electrical transfer and switching device was built with the $Ag_2S$ and Ag nanofiber bundles obtained from the chemical transformation of $Ag_2C_2O_4$ nanofiber bundles. The device configuration (indium tin oxide (ITO)/Ag/$Ag_2S$/ITO) is shown in Figure 8a, while the measured current–voltage (*I–V*) curve is shown in Figure 8b. When the voltage applied on the ITO electrode beside Ag nanofiber bundles was negative, the resistance was pretty high (~500 Ω) due to the low conductivity of $Ag_2S$, and the device was in its "off" state. After sweeping the voltage to the positive range, the $Ag^+$ ions in $Ag_2S$ nanofiber bundles near the ITO electrode began to be reduced and gradually formed an Ag filament towards the Ag nanofiber bundles; simultaneously, Ag on the Ag/$Ag_2S$ interface were oxidized and dissolved into $Ag_2S$ (Fig. 8c). The current significantly and rapidly increased when the Ag filament touched the Ag nanofiber bundles, and the device switched to its "on" state with a low resistance (~20 Ω). The transition from "off" to "on" occurred at 0.15 V. The above redox reaction reversed when the voltage swept back to the negative range and the device would switch off when the Ag filament broke from the Ag nanofiber bundles (Fig. 8d). The transition from "on" to "off" occurred at −1.7 V. Since the device was not symmetrical in structure, its *I–V* curve exhibited an obvious hysteresis.

While similar devices were reported for Ag/$Ag_2S$ heterostructure nanowires prepared in AAO membranes[25] and Ag-rich silver sulfide films,[35] our device was fabricated with layers of flat-lying nanofibers. It is demonstrated in our experiment that electrical transferring and $Ag^+$ ion migration can occur at physical-contact Ag/$Ag_2S$ interface, which might allow signal switching at the cross point of individual $Ag_2S$ and Ag nanofiber bundles. With the development of nanowire aligning and patterning techniques,[36] network of vertically crossed $Ag_2S$ and Ag nanofiber bundles could potentially act as high-capacity information storage and memory device. Moreover, compared with the platinum substrate and tungsten probe configuration employed in the literature,[25,35] two terminals in our device were built with ITO glasses, which was cost effective and scalable. Hence, our results demonstrated the potential applications of the $Ag_2S$ and Ag nanofiber bundles obtained from sacrificial template synthesis in fabrication of electrical transferring and switching devices with new configurations.

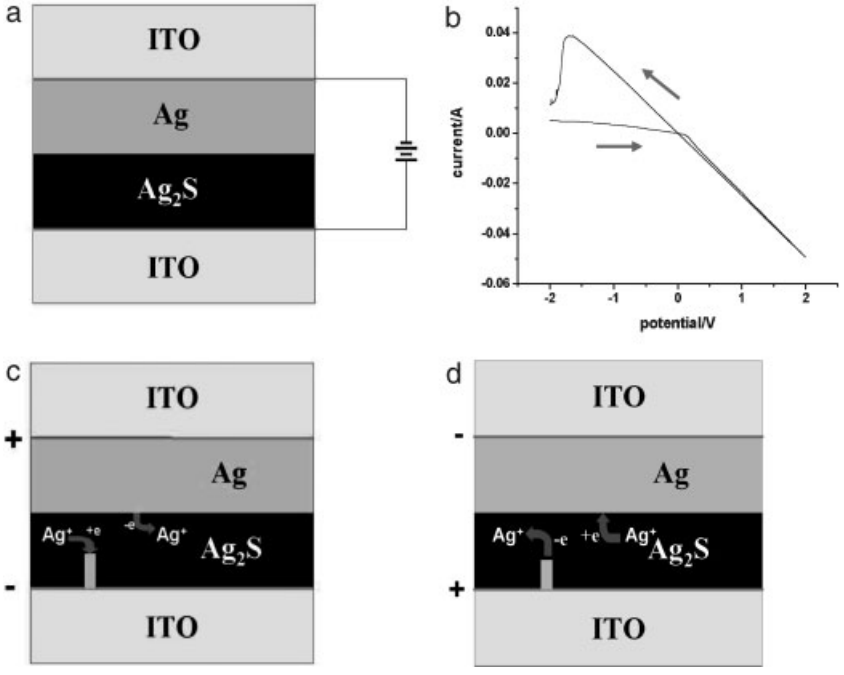


**Figure 8.** a) Schematic structure of the ITO/Ag/$Ag_2S$/ITO device, and b) its *I–V* curve. c,d) Schematic drawings of the operating mechanism.

ADVANCED FUNCTIONAL MATERIALS



If $Ag_2S$ nanofibers were replaced with $Ag_2Se$ nanofibers in the device, namely with the ITO/Ag/$Ag_2Se$/ITO configuration, only linear *I–V* curve was observed in a cycle (Fig. S3), which was consistent with the electric property of $Ag_2Se$ nanowires.[26] Under room temperature, $Ag_2Se$ usually takes $\beta$-phase and $Ag^+$ ion can not diffuse freely in the crystal.[14b,26] The lack of $Ag^+$ ion migration prohibited the electrical switching behavior in the Ag/$Ag_2Se$ device, indicating that the mixed-conductor nature of $Ag_2S$ is a key point for the switching device of Ag/$Ag_2S$.

## 3. Conclusions

With $Ag_2C_2O_4$ nanofiber bundles as a general sacrificial template, nanofiber bundles of $Ag_2S$, $Ag_2Se$, and Ag were successfully synthesized. The combination of anion exchange and redox reactions extended the range of products that could be obtained from a single template. While all the obtained nanofiber bundles were 1D nanoparticle assemblies with a polycrystalline nature, the Ag nanofiber bundles maintained the preferential orientation of the $Ag_2C_2O_4$ template. A fast transformation reaction between $Ag_2C_2O_4$ and a suitable reactant was essential for the morphology-preserved conversion or the templating synthesis of silver-based nanofiber bundles. It was indicated that $Ag_2C_2O_4$ nanofiber bundles were a general sacrificial template for the synthesis of silver-based semiconductor and metal nanofibers and the obtained 1D nanoparticle assemblies are likely to play critical roles in the improvement of the efficiencies of various devices.[37] An electronic device was built with $Ag_2S$ and Ag nanofiber bundles, the switching behavior resulting from $Ag^+$/Ag redox and $Ag^+$ ion diffusion revealed the potential application of the synthesized nanofiber bundles in memory device.

## 4. Experimental

*Synthesis of $Ag_2C_2O_4$ Nanofibers and Their Transformation*: In a typical synthesis of $Ag_2C_2O_4$ nanofiber bundles, 4.2 mL of $H_2O$, 0.5 mL of PAA (5g $L^{-1}$), and 50 μL of $Na_2C_2O_4$ (0.1 M) were mixed in a glass tube, to which 0.25 mL of $AgNO_3$ (0.2 M) was added under vigorous stirring. The glass tube was then kept still for 8 h and the products were collected by centrifugation and washed with water.

For synthesis of $Ag_2S$ nanofiber bundles, $Ag_2C_2O_4$ nanofiber bundles from one glass tube were dispersed in 5 mL of ethanol, to which 100 μL of TAA (0.1 M) was added under vigorous stirring.

For synthesis of $Ag_2Se$ nanofiber bundles, $Ag_2C_2O_4$ nanofiber bundles from one glass tube were dispersed in 5 mL of water, to which 50 μL of $Na_2SeSO_3$ (0.2 M) was added under vigorous stirring. $Na_2SeSO_3$ solution was prepared according to the literature [38].

For synthesis of Ag nanofiber bundles, $Ag_2C_2O_4$ nanofiber bundles from one glass tube were dispersed in 5 mL of water, to which 100 μL of $NaBH_4$ (0.1 M) was added under vigorous stirring.

For synthesis of separate Ag nanofibers, $Ag_2C_2O_4$ nanofiber bundles from one glass tube were dispersed in 20 mL of water and cooled to 4 °C, to which 50 μL of Vc (0.1 M) was added under stirring. The temperature was kept 4 °C for this reaction.

*Fabrication of the ITO/Ag/$Ag_2S$/ITO Device*: The nanofiber bundles of Ag and $Ag_2S$ were dispersed in water and coated on the higher-electrical-conductivity facet of ITO glasses with a thickness of several hundred micrometers, respectively. After naturally dried in air, two parts of the device were fixed with a clincher following the schematic structure in Figure 8a.

*Characterization*: The products were characterized by SEM (Hitachi S-4800), TEM (JEOL JEM-200CX), HRTEM (Hitachi H-9000HAR, FEI TECNAI F30), XRD (Rigaku Dmax-2000 with Cu K$\alpha$ irradiation), and UV-vis (Perkin-Elmer Lambda 35 UV-vis Spectrometer). The electrical measurement of the device was performed on an electrochemistry work station (CHI 660C).

Received: August 21, 2007
Revised: September 21, 2008
Published online: April 9, 2008

[1] K. J. C. van Bommel, A. Friggeri, S. Shinkai, *Angew. Chem. Int. Ed.* **2003**, *42*, 980.
[2] Y. Xia, P. Yang, Y. Sun, Y. Wu, B. Mayers, B. Gates, Y. Yin, F. Kim, H. Yan, *Adv. Mater.* **2003**, *15*, 353.
[3] S. J. Hurst, E. K. Payne, L. Qin, C. A. Mirkin, *Angew. Chem. Int. Ed.* **2006**, *45*, 2672.
[4] a) Y. Sun, Y. Xia, *Science* **2002**, *298*, 2176. b) Y. Yin, R. M. Rioux, C. K. Erdonmez, S. Hughes, G. A. Somorjai, A. P. Alivisatos, *Science* **2004**, *304*, 711.
[5] Y. Wu, T. Livneh, Y. Zhang, G. Cheng, J. Wang, J. Tang, M. Moskovits, G. D. Stucky, *Nano Lett.* **2004**, *4*, 2337.
[6] X. Yu, Y. Lee, R. Furstenberg, J. O. White, P. V. Braun, *Adv. Mater.* **2007**, *19*, 1689.
[7] N. Zhao, L. Qi, *Adv. Mater.* **2006**, *18*, 359.
[8] a) S. Yu, H. Cölfen, *J. Mater. Chem.* **2004**, *14*, 2124. b) A.-W. Xu, M. Antonietti, H. Cölfen, Y.-P. Fang, *Adv. Funct. Mater.* **2006**, *16*, 903. c) D. Zhang, L. Qi, J. Yang, J. Ma, H. Cheng, L. Huang, *Chem. Mater.* **2004**, *16*, 872. d) J. Bai, Y. Qin, C. Jiang, L. Qi, *Chem. Mater.* **2007**, *19*, 3367.
[9] Z. Li, S. Chung, J. Nam, D. S. Ginger, C. A. Mirkin, *Angew. Chem. Int. Ed.* **2003**, *42*, 2306.
[10] C. Mao, D. J. Solis, B. D. Reiss, S. T. Kottmann, R. Y. Sweeney, A. Hayhurst, G. Georgiou, B. Iverson, A. M. Belcher, *Science* **2004**, *303*, 213.
[11] A. Sugunan, P. Melin, J. Schnürer, J. G. Hilborn, J. Dutta, *Adv. Mater.* **2007**, *19*, 77.
[12] D. H. Son, S. M. Hughes, Y. Yin, A. P. Alivisatos, *Science* **2004**, *306*, 1009.
[13] a) H. Niu, M. Gao, *Angew. Chem. Int. Ed.* **2006**, *45*, 6462. b) S. Porel, N. Hebalkar, B. Sreedhar, T. P. Radhakrishnan, *Adv. Funct. Mater.* **2007**, *17*, 2550.
[14] a) B. Gates, Y. Yin, Y. Xia, *J. Am. Chem. Soc.* **2000**, *122*, 12582. b) B. Gates, Y. Wu, Y. Yin, P. Yang, Y. Xia, *J. Am. Chem. Soc.* **2001**, *123*, 11500.
[15] J. Yang, L. Qi, C. Lu, J. Ma, H. Cheng, *Angew. Chem. Int. Ed.* **2005**, *44*, 598.
[16] S. Jiao, L. Xu, K. Jiang, D. Xu, *Adv. Mater.* **2006**, *18*, 1174.
[17] H. Tong, Y. Zhu, L. Yang, L. Li, L. Zhang, *Angew. Chem. Int. Ed.* **2006**, *45*, 7739.
[18] Y. Sun, B. T. Mayers, Y. Xia, *Nano Lett.* **2002**, *2*, 481.
[19] Q. Lu, F. Gao, D. Zhao, *Angew. Chem. Int. Ed.* **2002**, *41*, 1932.
[20] X. Wen, S. Wang, Y. Xie, X. Li, S. Yang, *J. Phys. Chem. B* **2005**, *109*, 10100.
[21] C. Liang, K. Terabe, T. Hasegawa, M. Aono, *Solid State Ionics* **2006**, *177*, 2527.

  

[22] a) M. Kobayashi, *Solid State Ionics* **1990**, *39*, 121. b) U. Jeong, P. H. C. Camargo, Y. H. Lee, Y. Xia, *J. Mater. Chem.* **2006**, *16*, 3893.
[23] J. Chen, B. J. Wiley, Y. Xia, *Langmuir* **2007**, *23*, 4120.
[24] K. Terabe, T. Hasegawa, T. Nakayama, M. Aono, *Nature* **2005**, *433*, 47.
[25] C. Liang, K. Terabe, T. Hasegawa, R. Negishi, T. Tamura, M. Aono, *Small* **2005**, *1*, 971.
[26] D. T. Schoen, C. Xie, Y. Cui, *J. Am. Chem. Soc.* **2007**, *129*, 4116.
[27] B. J. Wiley, Z. Wang, J. Wei, Y. Yin, D. H. Cobden, Y. Xia, *Nano Lett.* **2006**, *6*, 2273.
[28] X. S. Peng, G. W. Meng, J. Zhang, X. F. Wang, L. X. Zhao, Y. W. Wang, L. D. Zhang, *Mater. Res. Bull.* **2002**, *37*, 1369.
[29] N. Du, H. Zhang, H. Sun, D. Yang, *Mater. Lett.* **2007**, *61*, 235.
[30] J.-F. Zhu, Y.-J. Zhu, M.-G. Ma, L.-X. Yang, L. Gao, *J. Phys. Chem. C* **2007**, *111*, 3920.
[31] P. Silvert, R. Herrera-Urbinab, K. Tekaia-Elhsissena, *J. Mater. Chem.* **1997**, *7*, 293.
[32] L. Zhao, K. L. Kelly, G. C. Schatz, *J. Phys. Chem. B* **2003**, *107*, 7343.
[33] D. Zhang, L. Qi, J. Ma, H. Cheng, *Chem. Mater.* **2001**, *13*, 2753.
[34] a) Y. Sun, Y. Xia, *Adv. Mater.* **2002**, *14*, 833. b) Y. Sun, B. Gates, B. Mayers, Y. Xia, *Nano Lett.* **2002**, *2*, 165.
[35] M. Kundu, K. Terabe, T. Hasegawa, M. Aono, *J. Appl. Phys.* **2006**, *99*, 103501.
[36] a) Y. Huang, X. Duan, C. M. Lieber, *Small* **2005**, *1*, 142. b) G. Yu, A. Cao, C. M. Lieber, *Nat. Nanotechnol.* **2007**, *2*, 372.
[37] Z. Tang, N. A. Kotov, *Adv. Mater.* **2005**, *17*, 951.
[38] Y. Ma, L. Qi, J. Ma, H. Cheng, *Adv. Mater.* **2004**, *16*, 1023.